ARCHIVE OF MECHANICAL ENGINEERING

DOI: 10.24425/ame.2023.144816 2023, Vol. 70, No. 1, pp. 107–128

Łukasz KUCZEK [1], Marcin MROCZKOWSKI [1], Paweł TUREK[1]

Investigation of deep drawability of 6082 aluminium alloy sheet for automotive applications after various heat treatment conditions

Received 10 August 2022, **Revised** 20 January 2023, **Accepted** 25 January 2023, **Published online** 10 February 2023

Keywords: 6082 alloy, drawability, heat treatment, mechanical properties, plastic anisotropy

The automotive industry requires more and more light materials with good strength and formability at the same time. The answer to this type of demands are, among others, aluminium alloys of the 6xxx series, which are characterized by a high strength-to-weight ratio and good corrosion resistance. Different material state can affect formability of AlMgSi sheets. These study analysed the influence of heat treatment conditions on the drawability of the sheet made of 6082 aluminium alloy. The studies on mechanical properties and plastic anisotropy for three orientations (0, 45, 90°) with respect to the rolling direction were carried out. The highest plasticity was found for the material in the 0 temper condition. The influence of heat treatment conditions on the sheet drawability was analysed using the Erichsen, Engelhardt-Gross, Fukui and AEG cupping tests. It was found that the material state influenced the formability of the sheet. In the case of bulging, the sheet in the annealed state was characterized by greater drawability, and in the deep drawing process, greater formability was found for the naturally aged material.

1. Introduction

Stamping is one of the 5 main groups of plastic forming processes for metals. It is possible to make thin-walled three-dimensional products from sheets, tapes or foils. Products such as cups, cans or structural elements (e.g., B pillar) and external panels of cars can be made. One of parameters describing the formability in the stamping processes is the drawability of sheets. The very term drawability can be defined, by citing [1], as "technological suitability of the material for plastic forming,

✉ Łukasz KUCZEK, e-mail: lukasz.kuczek@agh.edu.pl

[1] AGH University of Science and Technology, Faculty of Non-Ferrous Metals, Cracow, Poland.
ORCIDs: Ł.K. 0000-0003-0253-0673; M.M. 0000-0002-0870-6839

determining its ability to withstand large plastic deformations and the ease of adopting the desired shape in a specific stamping operation". This means that there is no universal test to conclude that a given material has better drawability than another. The drawability of the sheet depends both on properties of the material itself and on the deformation conditions in a specific technological operation [2–4]. During the analysis of the sheets drawability, a number of different types of technological cupping tests are performed [1, 5–8]. They are often replenished with the measurement of mechanical properties, strain hardening index and plastic anisotropy depending on the sample orientation in relation to the rolling direction (0, 45, 90°).

6xxx aluminium alloys are often used in the automotive, aerospace, and shipbuilding industries [9–13]. This is due, inter alia, to the good strength-to-density ratio, good mechanical properties and corrosion resistance [14] as well as the perfect balance between deformability and roping performance [9]. The chemical composition of 6xxx alloys significantly affects their properties. The higher content of alloying elements contributes to the formation of additional strengthening phases in alloys [15, 16]. These phases occur as a result of the performed heat treatment, conditions of which significantly affect both mechanical properties and the structure of the alloy [17–20]. Compared to the 5xxx series alloys, AlMgSi alloys are characterized by a lower deformability. Thus, 6xxx alloys are widely used as car panels, where dent resistance is one of the important factors [9, 21]. On the other hand, some of AlMgSi alloys are characterized by such a good drawability and stretch behaviour that they can also be used for elements that require high formability [14]. 6xxx alloys are also ideal in applications where high strength is required and deformability can be at an average level – for example in elements of the body structure of a car.

The most commonly used aluminium alloys of 6xxx series in the automotive industry are, among others, 6111, 6063, 6016, 6005A alloys [14]. Another material that can be used, for example, for load bearing framework of cars, is 6082 aluminium alloy. This is due to its very good strength (the highest among the 6xxx series alloys in T6 temper) and high corrosion resistance [22]. 6082 aluminium alloy also has some of the best impact resistance. At the same time, it has relatively good deformability. In the literature, one can find studies related to the analysis of heat treatment conditions for the structure, properties and corrosion resistance of 6082 aluminium alloy. The influence of the type of heat treatment on the material properties and the fracture toughness of 6082 alloy were analysed in the works [17, 18]. Based on the analysis of the results, the best ageing conditions were determined for which both notch-tensile strength and critical stress intensity factor were the highest. It was also noted that the cracks were initiated in void clusters and the primary areas of their nucleation were the separation of intermetallic phases. In [23], it was found that the dissolution of anodic phases in the matrix had a beneficial effect on the overall corrosion of the metal. On the other hand, natural and artificial ageing has a positive effect on the hardness and strength [17, 18, 24]. The authors in [25] analysed the combined effect of heat treatment, temperature and strain rate on formability of alloy 6082 in two different material states (0, T6).

It was found that the material after annealing was characterized by better plasticity, especially at a higher temperature and at a lower strain rate. In the case of the material after artificial ageing, the elongation increased up to a certain temperature, and then decreased. The authors found the greatest influence of the strain rate for the temperature of about 200°C. In [26] the influence of thickness on the formability of the 6082 alloy in the T6 state was analysed. It was found that the tensile strength and elongation increased with the thickness of the material while the yield strength decreased. The influence of the sheet thickness on the position of the limit deformation curve in the $\varepsilon_{\text{minor}}$-$\varepsilon_{\text{major}}$ system was also analysed. Higher formability was found for the sheet of greater thickness. The drawability of 6082 sheet was also analysed in works [1, 5]. In both cases, the material was validated only in the annealed condition. It was found that the tested sheet was characterized by good mechanical properties and good susceptibility of the material to stretching or bulging processes. As in [26], it was observed that the formability of the 6082 alloy sheet (in the 0 temper) was greater for the material thickness equal to 2 [mm] [5]. In the work [27] the analysis of stamping of cylindrical cups of 6082 T6 and 5754 H11 aluminium alloys was carried out. AlSi1MgMn alloy had higher strength and lower plasticity than $AlMg_3$ alloy. This translated into higher values of the forming force of the 6082 T6 sheet. Despite better plasticity and the slightly lower planar anisotropy index, the height profile of 5754 H11 drawpiece was similar to the harder material cups, both in terms of the position of the ears and their value. In paper [28], materials intended for stamping the Engine Oil Pan, including 6082 aluminium alloy sheet, were analysed. The lowest force stresses in the total deep drawing and punching forces occurred on Al 6082. At the same time, it was noted that for this material the initial sheet thickness was extremely important, compared to the other analysed alloys.

There is a limited number of studies in which the deep drawing process of 6082 aluminium alloy has been investigated comparatively under different temper conditions. Moreover, some drawing tests simulate the actual conditions of the sheet forming processes (e.g., Erichsen, Engelhardt-Gross and AEG cupping test). Therefore, depending on the test and heat treatment, the sheet may have different drawability. The relationship between drawability and heat treatment has not yet been widely analysed. This work investigates the influence of the heat treatment conditions on the drawability of the sheet made of the EN AW-6082 aluminium alloy. Mechanical properties and plastic anisotropy of the sheet were determined. The drawing coefficients were measured on the basis of four methods: Erichsen, Engelhardt-Gross, Fukui and AEG cupping test.

2. Research methodology

Generally, in the automotive industry, sheets with the thickness of 0.9 to 3 mm are used. In this work, 6082 sheet with the thickness of 2 mm was used for the tests. The chemical composition of aluminium alloy, determined using the spark

spectrometer FOUNDRY-MASTER Xpert, is given in Table 1. The material was delivered in F temper. The influence of heat treatment conditions on the drawability of the sheet was investigated. For this purpose, a tensile test and a number of technological drawing tests were carried out. The heat treatment conditions of EN AW-6082 aluminium alloy are shown in Table 2.

Table 1. Chemical composition of the tested sheet made of the EN AW-6082 alloy

Al	Si	Mg	Mn	Cu	Fe	Zn	Cr	Ti
Rest	1.037	0.558	0.449	0.059	0.519	0.073	0.032	0.046

Table 2. Heat treatment conditions of 6082 sheet [18, 24]

Material state	Heat treatment condition
0 (annealed)	575°C/2 h; cooled with oven
S (supersaturated)	575°C/2 h cooled in water (25°C)
T4 (natural ageing)	20°C/500 h
T6 (artificial ageing)	190°C/6 h

The tensile test was carried out according to the requirements of the ISO 6892-1 standard with the constant strain rate equal to $1 \cdot 10^{-3}$ s^{-1}. The width and length of the gauge were 12.5 mm and 50 mm, respectively. The tests were carried out for three sample orientations in relation to the rolling direction of the sheet: 0, 45 and 90°. The material strength (YS, UTS) and plastic properties (A_g, A_{50mm}) were determined. The plastic anisotropy for various material states was tested under the test conditions specified in the standard ISO 10113. The values of the Lankford coefficient (R) for a given orientation were calculated according to the equation [1, 5, 20, 29]:

$$R = \frac{\varepsilon_w}{\varepsilon_t} = \frac{\ln \dfrac{w_f}{w_0}}{\ln \dfrac{l_0 w_0}{l_f w_f}}, \tag{1}$$

where ε_t is the true plastic thickness strain, ε_w is the true plastic width strain, w_0 and l_0 are the original gauge width and length of the test piece, respectively, w_f and l_f are gauge width and length of the test piece after straining to specified plastic elongation. Mean values of R_{av} were determined, as well as the planar anisotropy index ΔR, according to equations [1, 5, 20, 29]:

$$R_{av} = \frac{R_0 + 2R_{45} + R_{90}}{4}, \tag{2}$$

$$\Delta R = \frac{R_0 + R_{90} - 2R_{45}}{2}, \tag{3}$$

where R_0, R_{45} and R_{90} are Lankford coefficients for three different directions of loading in-plane (0, 45, 90° to the rolling direction).

Technological drawability tests included four methods: Erichsen, Engelhardt-Gross, Fukui and AEG cupping tests (also known in the literature as the rapid determination method RDM [30]). Tests were carried out on the Erichsen model 142/40 universal machine for testing sheets and strips. In the case of the Erichsen test, three measurements were made for each material condition. In the other tests, at least five specimens were used. On the basis of the measurement of the drawpieces height (on the samples obtained in the AEG cupping test), the technological planar anisotropy coefficients for 6082 sheet were additionally determined.

The Erichsen test (Fig. 1), which determine the stretch-forming capacity of sheets and strips, was carried out according to the recommendations of the ISO 20482 standard. In this test, the sample 100 mm wide and 300 mm long was clamped between the die and the sheet holder with the load equal to 10 kN. The distance travelled by the punch (with a diameter equal to 20 mm) until a continuous crack appeared through the sheet was measured. The distance of the first bulge from the edge was 50 mm. The successive measurement points were approximately 100 mm apart. In total, three measurements were made for each sample. The test was performed at the punch feed rate of 10 mm/min with the use of graphite grease.

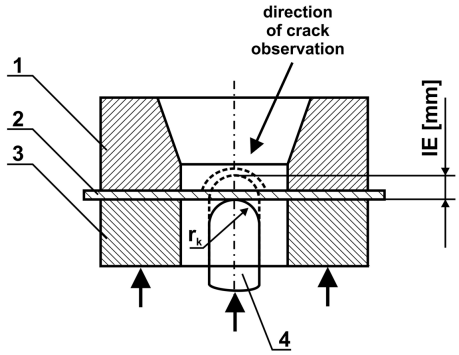

Fig. 1. Scheme of Erichsen cupping test
1 – die, 2 – sheet, 3 – sheet holder, 4 – punch

The Engelhardt-Gross test (Fig. 2), which simulated deep drawing process, was conducted in two stages. In the first stage, cylindrical cups with a flange were stamped, during which the maximum drawing force F_{max} was measured. The test was carried out on dies with smooth edges with a blankholding force (BHF) of 2 kN. Graphite grease was used during stamping. In the second stage of the Engelhardt-Gross test, in which the tearing force F_t was measured, the die with a serrated edge of the die opening was used. At the same time, the flange was clamped between the die and the blank holder with the BHF equal to 20 kN. The test was carried out without a lubricant. In both stages, the same punch speed of 10 mm/min was used.

Engelhardt coefficient T was calculated according to the equation [1]:

$$T = \frac{F_t - F_{\max}}{F_t} \cdot 100\% \tag{4}$$

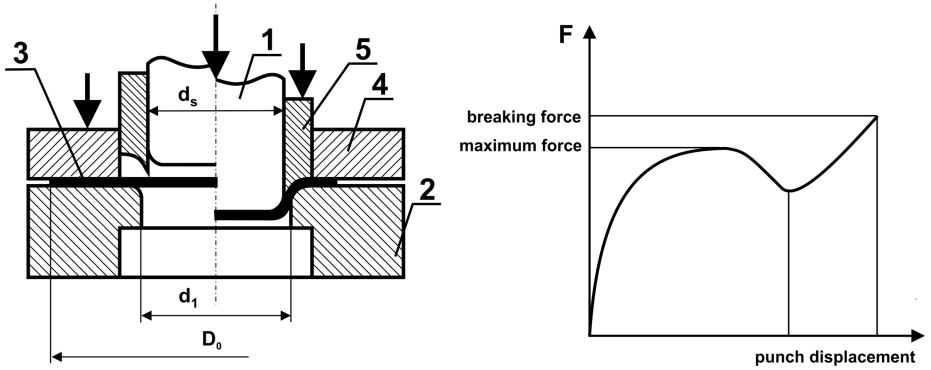

(a) (b)

Fig. 2. Scheme of Engelhardt-Gross test (a) and graph of the dependence of the drawing force on the displacement of the punch during the test (b)
1 – punch, 2 – die, 3 – blank, 4 – blankholder for maximum force measurement stage, 5 – additional blankholder for tear force measurement stage

In the Fukui test (Fig. 3), conical cups were stretched and pulled until the continuous through crack appeared at the top of the drawpiece. In this type of test, lubrication, bending of the material on the die edge, and the blankholding force have no effect on the process of forming the cups. The punch speed of 50 mm/min and diameter of blank equal to 78 mm were used. After the test, the maximum and minimum diameters of the conical cups were measured. The equation for Fukui

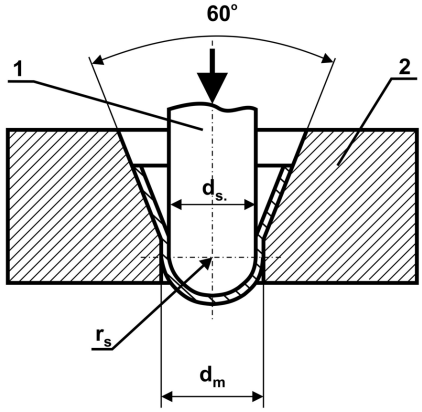

Fig. 3. Scheme of Fukui test; 1 – punch, 2 – conical die

index η_F is shown below [1, 2]:

$$\eta_F = \frac{d_{\max} - d_{\min}}{2D_0}, \tag{5}$$

where D_0 is the original blank diameter, $d_{\max}$ and $d_{\min}$ are the maximum and minimum diameters of the conical cup, respectively.

In the AEG cupping test (Fig. 4a), stamping of cylindrical cups from blanks with three different diameters D (40, 50 and 70 mm) was carried out [1, 30]. The constant value of the blankholding pressure equal to 1 MPa was used. The punch with the diameter d of 32 mm and graphite grease as lubricant were used in the test. In the case of the blanks for which defect-free cups were obtained (40 and 50 mm), the maximum drawing forces $F_{\max}$ were measured. For the blank where tearing occurred (70 mm), the tearing force F_t was measured (F_t = const for d = const). Five drawpieces were made for each measuring point. To determine the limiting drawing ratio (LDR), the linear approximation of maximum drawing forces was used and extrapolated to the tearing force value (Fig. 4b). The point of intersection determined the value of LDR for each material state of the 6082 alloy sheet.

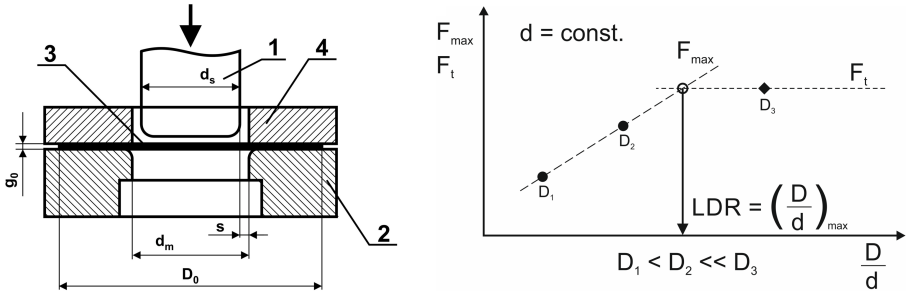

(a) (b)

Fig. 4. Schemes of AEG cupping tests (a) and method of determining LDR (b)

3. Results

3.1. Mechanical properties

Fig. 5 shows examples of sheet tensile curves for 6082 aluminium alloy after various heat treatment conditions. They represent the typical shape of the tensile curves for 6xxx alloys, without upper and lower yield point. The tensile curve for 6082 sheet after artificial ageing was characterized by the flattest plastic flow area, which at the same time correlated with a low value of the hardening exponent and a high YS/UTS ratio (Table 3). In the case of annealed sheet, the situation was the opposite. The hardening index was the highest (n = 0.26), while the YS/UTS ratio was the lowest (0.34).

Table 3. Mechanical properties of tested materials in different temper

EN AW-6082 "0"					
Sample orientation α [°]	Yield strength YS [MPa]	Ultimate tensile strength [MPa]	Elongation at break A_{50mm} [%]	Uniform elongation A_g [%]	Strain hardening index n
0	43.2	128.4	28.8	23.0	0.257
45	43.5	127.1	27.4	21.6	0.261
90	45.0	127.3	28.0	22.0	0.260
Mean value	**43.8**	**127.5**	**27.9**	**22.1**	**0.260**
EN AW-6082 "S"					
Sample orientation α [°]	Yield strength YS [MPa]	Ultimate tensile strength [MPa]	Elongation at break A_{50mm} [%]	Uniform elongation A_g [%]	Strain hardening index n
0	149.7	275.7	24.4	21.9	0.211
45	146.2	273.3	25.6	22.5	0.213
90	154.1	278.6	24.4	22.0	0.217
Mean value	**149.1**	**275.2**	**25.0**	**22.2**	**0.214**
EN AW-6082 "T4"					
Sample orientation α [°]	Yield strength YS [MPa]	Ultimate tensile strength [MPa]	Elongation at break A_{50mm} [%]	Uniform elongation A_g [%]	Strain hardening index n
0	151.0	281.6	26.8	23.6	0.208
45	150.9	279.2	26.4	23.2	0.206
90	151.0	280.4	26.8	22.4	0.215
Mean value	**151.0**	**280.1**	**26.6**	**23.1**	**0.209**
EN AW-6082 "T6"					
Sample orientation α [°]	Yield strength YS [MPa]	Ultimate tensile strength [MPa]	Elongation at break A_{50mm} [%]	Uniform elongation A_g [%]	Strain hardening index n
0	313.3	329.9	8.4	6.3	0.032
45	302.5	322.8	9.4	7.2	0.040
90	301.5	320.6	10.2	8.2	0.041
Mean value	**305.0**	**324.0**	**9.4**	**7.2**	**0.038**

The properties of the 6082 T4 sheet were similar to 6xxx aluminium alloys widely used in the automotive [14]. The yield strength, tensile strength as well as uniform elongation and elongation at break largely depend on the material state (Table 3). The lowest yield strength and an ultimate tensile strength were found for the annealed sheet and were 43.8 MPa and 127.5 MPa, respectively.

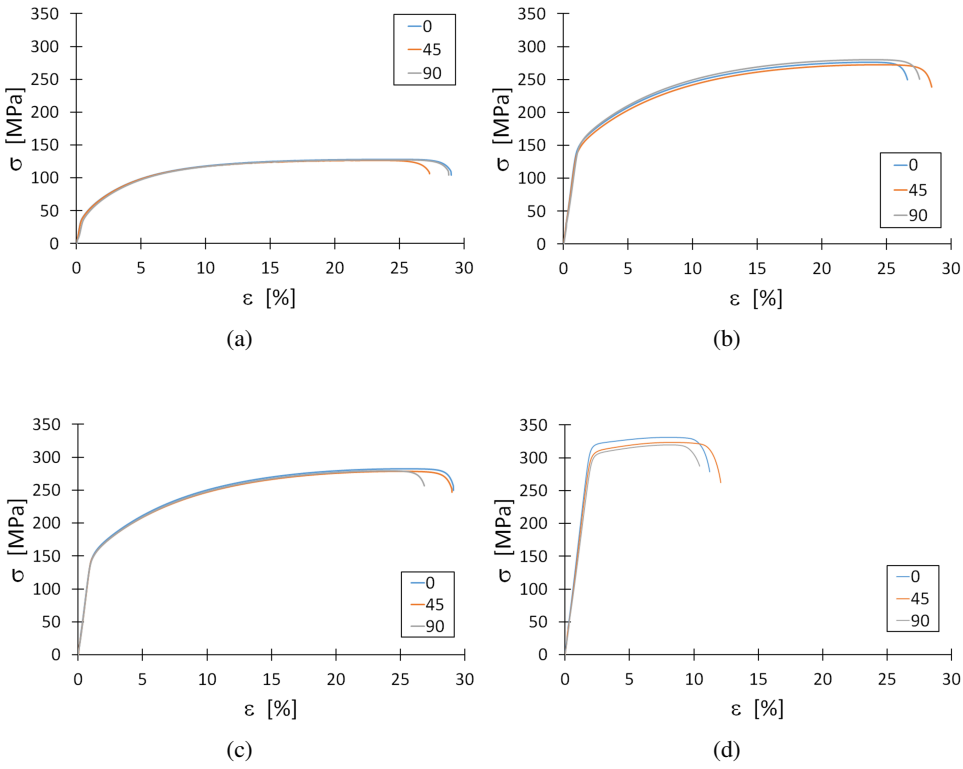

Fig. 5. Examples of stress-strain diagrams for 6082 sheet in various hardening conditions: (a) 0, (b) S, (c) T4, (d) T6

The mean elongation at break for this material was about 28% and it was the highest among the examined cases. Slightly lower plasticity was found for the sheets after supersaturation (S) and natural ageing (T4). Their elongations were equal to 25.0% and 26.6%, respectively. At the same time, the strength of 6082 aluminium alloy increased, although it was lower than in the case of the aluminium alloy after artificial ageing (Table 3). For the tested material in the T6 temper, the yield strength and tensile strength were equal to 305 MPa 324 MPa, respectively. At the same time, the elongation at break did not exceed 10%.

The sheet after artificial ageing showed the greatest differences in values of strength and elongation at break in the sheet plane (Fig. 6). For the 90° orientation, the values of these parameters were the highest. On the other hand, the sheet in the T6 temper had an even distribution of the uniform elongation and continuous decrease of $A_{50\text{mm}}$ from 0° to 90° (Fig. 6d). In the case of sheets in the 0, S and T4 temper, the distribution of $A_{50\text{mm}}$ was non-uniform. The central point (with the lowest or highest value) was the elongation determined for the 45° orientation with respect to RD.

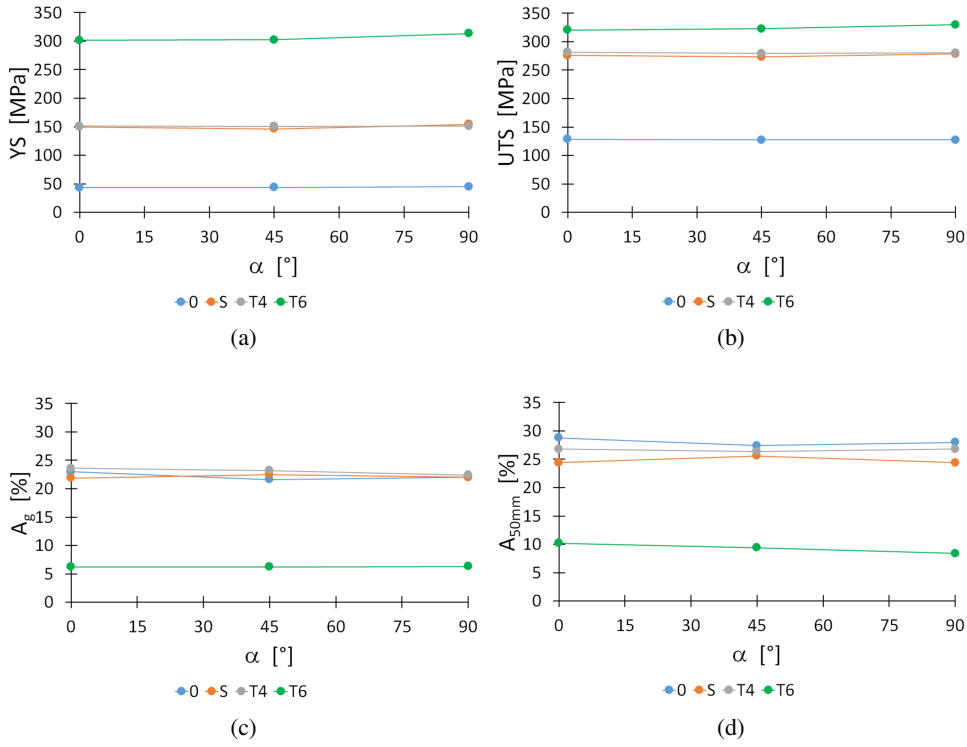

Fig. 6. Yield strength (a), tensile strength (b), uniform elongation (c), and elongation at break (d) in dependence of the sample orientation

3.2. Plastic anisotropy

The values of normal anisotropy coefficients for the tested sheet ranged from 0.53 to 0.60 (Table 4). The highest mean values of the Lankford coefficient were found for the sheet after natural ageing (0.596) and the lowest ones for the material after annealing (0.537). In all the analysed cases, the R-value was also found to depend on the direction of loading in-plane. In the case of the 45° direction, the Lankford coefficient values were the highest (from 0.546 for annealed material to 0.603 for 6082 alloy after natural ageing), regardless of applied conditions of the heat treatment (Fig. 7). The lowest R-values were recorded for the 0° direction (between 0.524 and 0.579). However, the differences between Lankford coefficients for various orientations were insignificant. This influenced planar anisotropy indexes. Their values did not exceed $\Delta R = -0.025$. This practically means a slight difference in the height of drawpieces measured along its circumference, with possible slight ears in 45° directions. This effect was also confirmed during the analysis of the technological planar anisotropy index of cups.

Table 4. Normal anisotropy and planar anisotropy coefficients

Hardening state	Sample orientation α [°]	R	ΔR
0	0	0.524	−0.018
	45	0.546	
	90	0.532	
	R_{av}	**0.537**	
S	0	0.536	−0.020
	45	0.560	
	90	0.544	
	R_{av}	**0.550**	
T4	0	0.579	−0.015
	45	0.603	
	90	0.598	
	R_{av}	**0.596**	
T6	0	0.530	−0.023
	45	0.558	
	90	0.547	
	R_{av}	**0.547**	

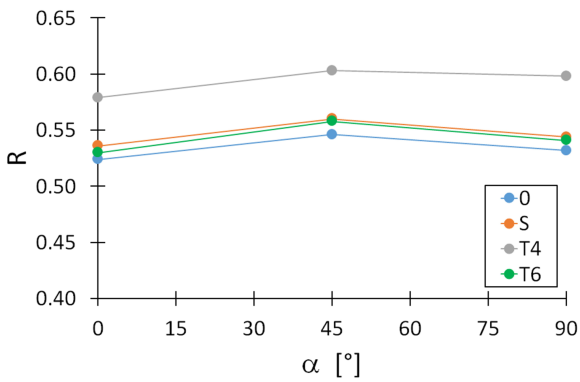

Fig. 7. Lankford coefficient in dependence of the sample orientation for different tempers of 6082 sheet

3.3. Technological cupping tests

Table 5 presents results of technological cupping tests performed on 6082 sheets after various heat treatment conditions. It was found that, depending on the type of test, the sheet had different drawability.

Table 5. Summary of cupping test results

Method	Test coefficient	Hardening state			
		0	S	T4	T6
Erichsen	IE [mm]	11.2	9.8	9.8	8.3
Fukui	η_F	0.838	0.848	0.851	0.879
Engelhard-Gross	T [%]	38.1	39.1	41.7	39.0
AEG cupping test (RDM)	LDR	2.04	2.27	2.33	2.08

Erichsen test

The Erichsen test allows for assessing the resistance of the sheet to cracking during biaxial stretching with the participation of friction on the face of the punch [1, 5]. The value of the Erichsen index for the tested sheet depended of material state (Fig. 8). The material after annealing, with the lowest strength, was characterized by the highest value of the Erichsen coefficient. This value was 11.2 mm and it was within the range known from the literature for this alloy and its material state [1, 5]. The lowest Erichsen index was obtained for the 6082 sheet after artificial ageing (with the highest strength), which was equal to 8.3 mm. In the case of the remaining samples, the values of the IE index were found at the level of 9.8 mm.

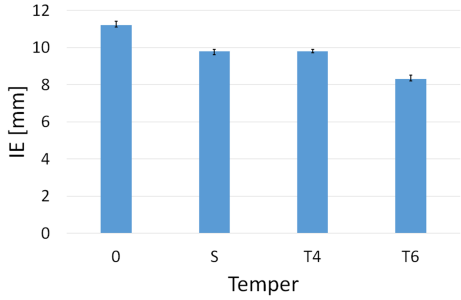

Fig. 8. Erichsen index for 6082 sheet at various material states

As in [5], while measuring the Erichsen index, the force F at which the continuous crack appeared was also measured (Fig. 9). The lowest value was found

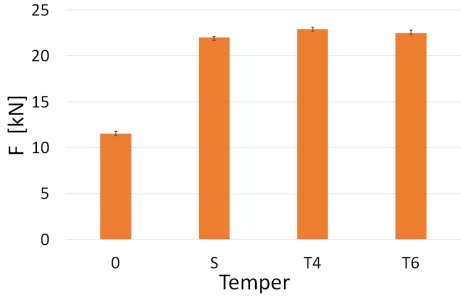

Fig. 9. The values of the fracture force obtained in Erichsen test

for the annealed sheet, which can be related to its low strength. It was almost two times lower than in the case of material after other heat treatment conditions. For these cases, the values of the cracking force were at a similar level and ranged from 22 [kN] to 23 [kN].

Fukui test

The Fukui test, unlike other technological cupping tests used in the work, does not simulate actual drawing processes. There is no influence of bending, friction, and blankholding force. It is characterized by high sensitivity and repeatability of results [1, 31]. Nevertheless, this test is rarely used in the analysis of sheet drawability. In the Fukui test, the lower the η_F index value, the better the drawability of the sheet. In the case of the tested heat treatment conditions, the material in the annealed state was characterized by the best drawability (Fig. 10. Its value was at the level of 0.84, slightly lower than that of the other material states. On the other hand, with the increase in the strength of 6082 aluminium alloy, the value of the index increased. The highest values of the Fukui index were determined for the sheet after artificial ageing ($\eta_F = 0.88$).

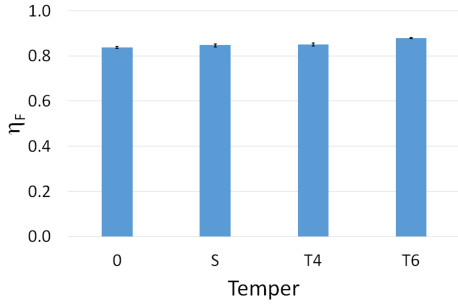

Fig. 10. Fukui η_F graph for 6082 sheet in different temper

Engelhardt-Gross test

The Engelhardt-Gross test, in terms of the state of stress and deformation, reflects the process of drawing of cylindrical cups [1, 32]. The values of the Engelhardt coefficient for the tested sheets ranged from 38 to 42% (Fig. 11a). The higher its value, the better the drawability of the sheet. In the case of the analysed sheets, the best drawability was demonstrated by the material after natural ageing ($T = 41.7\%$). On the other hand, for the annealed 6082 alloy, the T value was lower, equal to 38.1%. It was mainly related to a small difference between the value of the tearing force F_t, equal to 23.8 kN, and the maximum force $F_{\max}$, which was equal to 14.75 kN (Fig. 11b). On the other hand, the sheet at T4 was characterized by the greatest difference between them ($F_t = 58.4$ kN, $F_{\max} = 34.1$ kN, $\Delta F = 24.3$ kN). As a result, the Engelhardt coefficient for the sheet after natural ageing was the highest among the tested material states.

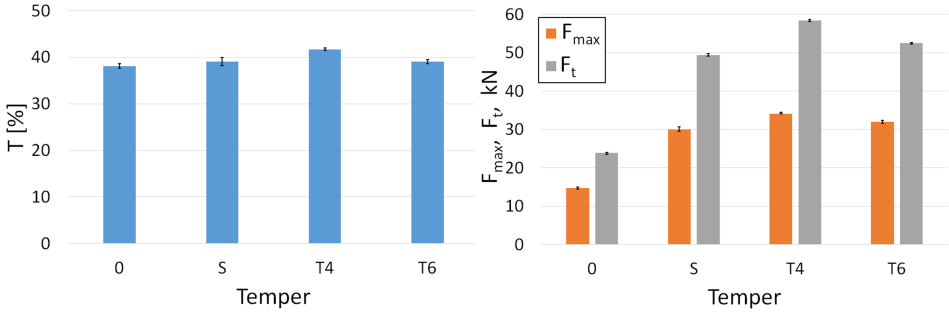

(a) (b)

Fig. 11. Engelhardt coefficient (a) and the tearing force and maximum force (b) values for 6082 sheet after various conditions of heat treatment

AEG cupping test

Application of the AEG cupping test (RDM) makes it possible to determine the limit drawing ratio LDR for cylindrical cups with the use of a small number of blanks [30]. Fig. 12 shows graphs of the relationship between the maximum drawing force and the LDR. Assuming a constant punch diameter, the tearing force value can be considered constant in this system (horizontal dashed line). Its value

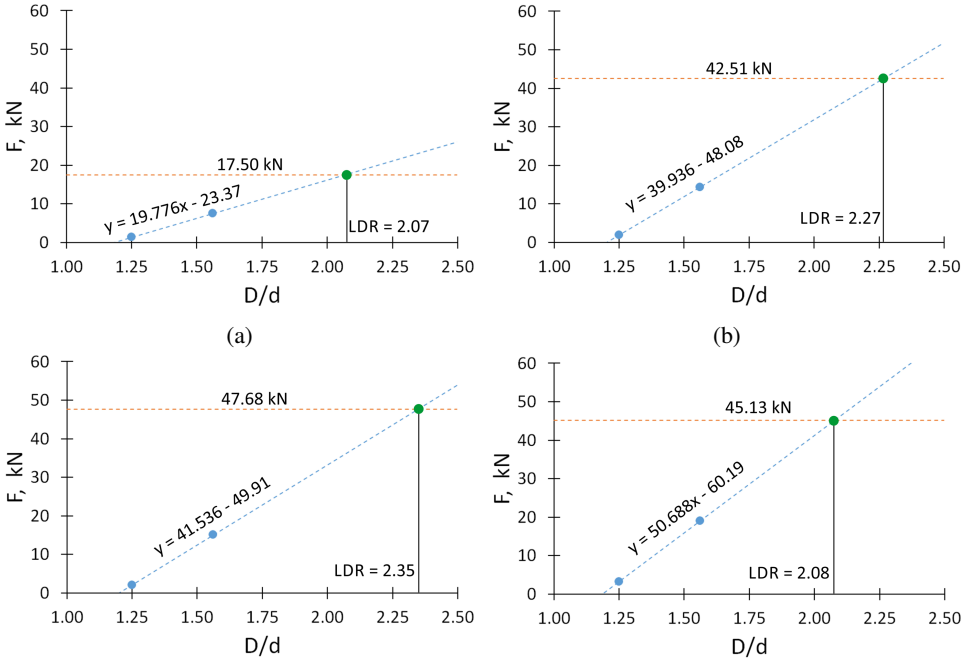

(a) (b) (c) (d)

Fig. 12. Diagram of the maximum drawing force and fracture force during the cupping test of 6082 sheets in the following condition: (a) 0,(b) S, (c) T4, (d) T6

depends on the material state. The highest value of F_t was recorded for the sheet after natural ageing. It was almost three times higher than for the annealed material. Based on the intersection of the diagrams, the limit values of the LDR for the sheet after a given heat treatment were determined (Table 6). The intersection of the graphs determines the cut-off point above which only shallow flanged cups can be formed.

Fig. 13 shows the diagram of LDR values for different 6082 tempers. The highest limit drawing ratio was characteristic for the sheet after natural ageing (2.33), while the lowest one appeared after annealing (2.04) and in the T6 temper (2.08). Despite a slightly lower value of the tearing force for the sheet after artificial ageing, about 45 kN compared to about 48 kN for T4 (Fig. 12c), this material was characterized by a large increase in the value of the maximum force along with the increase of the blank diameter (Fig. 12d). On the other hand, the combination of a small increase of the maximum drawing force with D/d (compared to other materials) and the low F_t (Fig. 12a) also led to low LDR value for the annealed sheet.

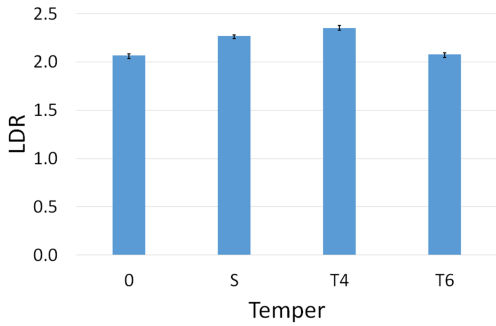

Fig. 13. Values of the LDR for 6082 sheet after various conditions of heat treatment

After conducting the cupping test, it was possible to measure the height of drawpieces along the circumference. The technological planar anisotropy index Z was calculated according to equation (6) [33]. It was found that the differences of the drawpiece height were insignificant. Hence, the values of the technological planar anisotropy index Z for the 6082 sheet did not exceed 0.33% (Fig. 14). These results correlate well with the values of the planar anisotropy index ΔR.

$$Z = \frac{h_e}{\bar{h}} 100\% \,, \tag{6}$$

where h_e $(= \bar{h}_p - \bar{h}_v)$ is the mean ears height, $\bar{h}$ $(= \dfrac{\bar{h}_p + \bar{h}_v}{2})$ is the mean cup height, $\bar{h}_p$, $\bar{h}_v$ are, respectively, average values of all ears and troughs of cup profile.

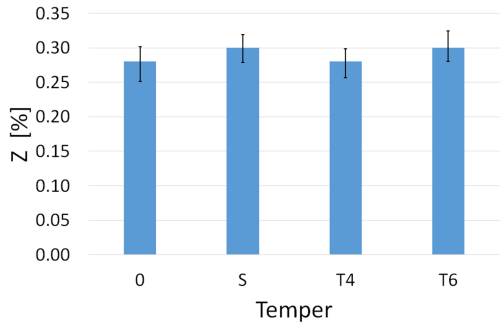

Fig. 14. The technological planar anisotropy coefficient in dependence of the material state of the 6082 aluminium alloy

4. Discussion

Due to the complex state of stress and deformation in stamping processes, it is necessary to analyse the sheet, both in terms of mechanical properties and drawability. In general, higher ductility of a material is associated with better formability. In the case of 6082 aluminium alloy, this relationship was reflected in the Erichsen and Fukui tests, i.e., where the biaxial state of tensile stresses in the sheet plane occurred. Greater plasticity of the annealed material contributed to obtaining deeper bulges in the sheet (Erichsen test) and higher cylindrical drawpieces (Fukui test). On the other hand, products made of 6xxx alloys are often artificially aged after deformation in order to increase their strength. To this end, a given element is first supersaturated and then aged in various temperature and time conditions [18]. It may be associated with various types of shape buckling, resulting from rapid cooling in water [34]. Hence, in some cases, it may be more advantageous to form the sheet in a supersaturated or T4 temper, despite the lower Erichsen index and the higher forces required for this type of forming. Such a product may then be subjected to additional heat treatment at a temperature not exceeding 200°C, which significantly improves its hardness [35]. Moreover, better effects of artificial ageing are achieved for a supersaturated element than in T4 temper [36].

In the Engelhardt-Gross test and the AEG cupping test, the annealed sheet was characterized by the lowest indexes, comparable to T6 temper. In these tests, the stress and deformation conditions are similar to those that occur during forming cylindrical cups - circumferential compression and radial stretching of the flange. This effect can also be related to the relatively high value of the hardening index, which has a positive effect on the material's resistance to cracking in such processes as bulging or uniaxial stretching. The opposite effect occurred in the case of the naturally aged sheet. Despite the higher strength, it was also characterized by a higher normal anisotropy coefficient and a better drawability indexes, determined on the basis of the Engelhardt-Gross and AEG cupping tests. The hardening exponent for this material state was lower than that of the annealed sheet. Although the

exponent value is not of great importance during the first step of deep drawing process, it significantly influences subsequent drawing operations. A lower value for the sheet in the T4 temper may contribute to the reduction in the number of the annealing processes necessary to eliminate the strain hardening effect of the material. On the other hand, too low value of n, combined with low plasticity and high value of the YS/UTS ratio, could contribute to worse results of the 6082 sheet in T6 temper in all technological cupping tests.

A similar relationship as in the case of elongation was also found for the normal anisotropy coefficient. Its high value increases drawability of the sheet [1, 37]. This is due to the fact that for a higher R-value the longitudinal deformation is more precisely compensated by the transverse deformation (the change of the sample width) than by the thickness reduction [38]. For the 6082 aluminium alloy, the sheet after natural ageing showed the best normal anisotropy coefficients. However, its value was still less than 1, which may make the sheet more suitable for use in processes such as bulging and stretching. On the other hand, the high LDR (2.33) and the T-index (41.7%) do not preclude the use of 6082 sheet in the T4 temper in the deep drawing process.

An important factor influencing the possibility of using the 6082 sheet in the stamping processes is the distribution of mechanical properties in the sheet plane. The presence or absence of significant differences in properties, especially the plastic ones, may be of great importance during stamping. This is especially true for the products with more complex shapes. A large difference in properties can cause a non-uniform material flow and hence the possibility of ears and large material losses. On the other hand, the even distribution of properties contributes to a more uniform material flow and a more even edge of the drawpiece. This effect was observed for all the material states of the 6068 sheet. The differences in values of strength and plastic parameters for different orientations were so negligible that they insignificantly affected the appearance of the drawpiece edge (Fig. 15). Both the planar anisotropy index Δr and the technological planar anisotropy index Z reached small values, close to zero, regardless of the applied heat treatment.

Fig. 15. The appearance of the exemplary (6082 T4) cup edge after drawing

In the Erichsen's test, it is also possible to perform a qualitative assessment of the sheet structure [1]. This is done on the basis of the organoleptic observation of the surface of the bulge and the crack. In the case of the analysed material, the surfaces of the bulges were relatively smooth, regardless of the applied heat treatment. Hence, it can be concluded that the tested sheets were characterized by a relatively fine-grained structure. However, the shape of the crack was different for different material states. In the case of annealed material, cracking occurred along the arc in the circumferential direction (Fig. 16a). However, in the remaining cases, this line diverged from the arc towards the bottom of the bulge (Figs. 16b–16d). Moreover, for the materials after ageing (natural and artificial) the crack was irregular, "serrated". This suggests that in the case of the sheet after annealing, the material was characterized by the best homogeneity of the structure, while for the sheets after ageing, this homogeneity could be disturbed. This effect may result, inter alia, from the presence of intermetallic phases in the material, which are the nucleation sites for voids [18].

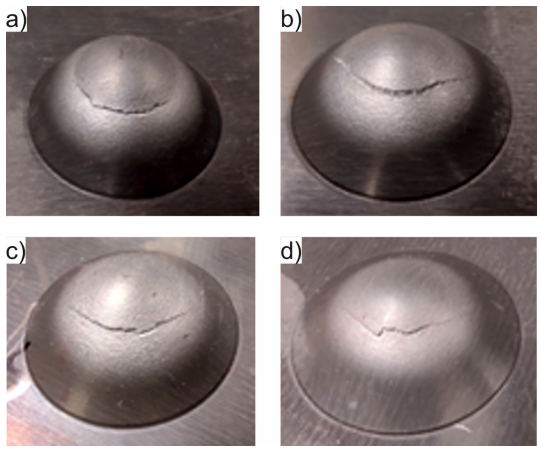

Fig. 16. The appearance of bulges after the Erichsen test for the 6082 aluminium alloy in: 0 (a), S (b), T4 (c) and T6 (d) temper

In the case of cupping tests, a relationship can be found between drawability coefficients and material strength (Fig. 17). In the Erichsen test, the Erichsen index decreased with the tensile strength of the material (Fig. 17a). However, in the case of the Fukui test, the value of the η_F coefficient also increased with the increase of the 6082 alloy strength (Fig. 17b). This means that in both cases the increase in the strength of the 6082 aluminium alloy resulted in a reduction in the drawability of the sheet. In the case of tests where compression stresses were the dominant ones, the coefficient values increased with the strength to the UTS level determined for the 6082 alloy in the T4 state (Fig. 17c, 17d). Then, their value decreased along with the increase in endurance.

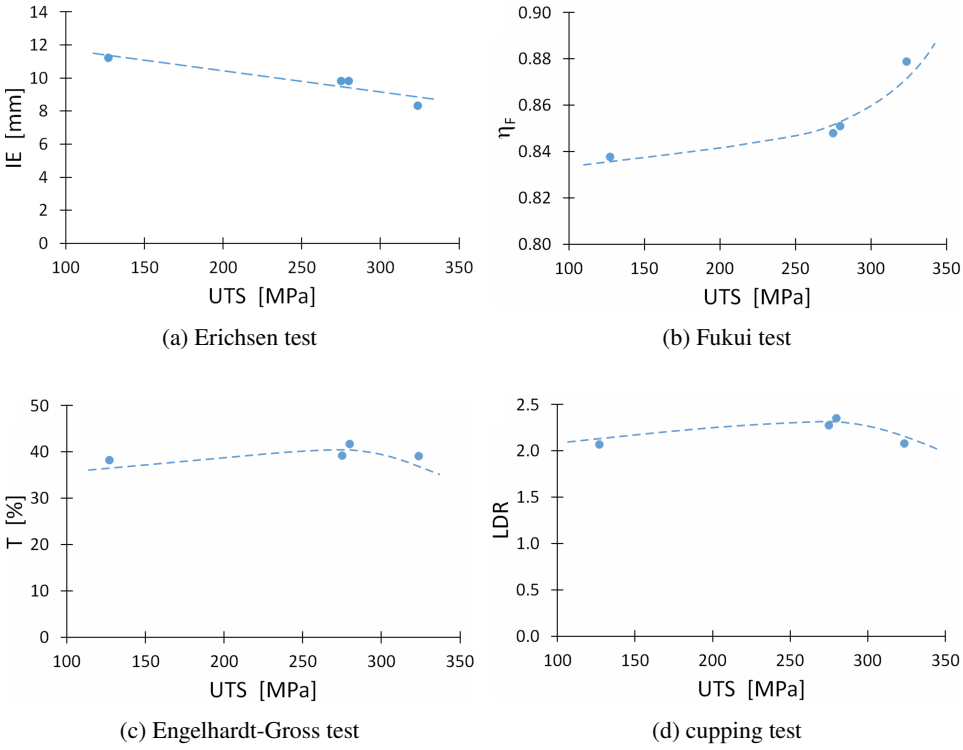

(a) Erichsen test

(b) Fukui test

(c) Engelhardt-Gross test

(d) cupping test

Fig. 17. Dependence of drawability coefficients on the material strength for various tests

5. Conclusions

This study analysed the influence of the material condition on the formability of the sheet, determined on the basis of the tensile test and technological drawing tests. It was found that, depending on the material states, the 6082 sheet was characterized by different drawability coefficients. Moreover, their values depended on the drawability test. The annealed sheet had the best plastic properties, the highest hardening index and the best coefficient values in the Erichsen and Fukui tests. On the other hand, 6082 aluminium alloy after natural ageing was characterized by the highest value of the normal anisotropy coefficient and the drawability indexes in the Engelhardt-Gross as well as AEG cupping tests. This means that for a given stamping process, it may be necessary to use a sheet in different material states. In the case of plastic forming of spherical, paraboloidal, conical, etc., elements, by means of dies with drawing thresholds or hydraulic bulging, the most suitable heat treatment of the 6082 sheet is annealing. On the other hand, in the case of deep drawing process, natural ageing of the sheet is definitely the most advantageous temper. In addition, the use of the sheet in T4 temper allows for further heat treatment of the product, without the risk of buckling during supersaturation.

Acknowledgments

This study was founded by the Faculty of Non-Ferrous Metals at AGH-University of Science and Technology in Krakow, Poland (Research Subsidy No 16.16.180.006).

References

[1] W. Muzykiewicz. Validation tests for the 6082-grade sheet in the "0" state with an account of its application for deep drawing processes. *Rudy i Metale Nieżelazne*, 51(7):422–427, 2006. (in Polish).

[2] A.C.S. Reddy, S. Rajesham, P.R. Reddy, and A.C. Umamaheswar. Formability: A review on different sheet metal tests for formability. *AIP Conference Proceedings*, 2269:030026, 2020. doi: 10.1063/5.0019536.

[3] Y. Dewang, V. Sharma, and Y. Batham. influence of punch velocity on deformation behavior in deep drawing of aluminum alloy. *Journal of Failure Analysis and Prevention*, 21(2):472–487, 2021. doi: 10.1007/s11668-020-01084-5.

[4] S. Bansal. *Study of Deep Drawing Process and its Parameters Using Finite Element Analysis*. Master Thesis, Delhi Technological University, India, 2022.

[5] E. Nghishiyeleke, M. Mashingaidze, and A. Ogunmokun, Formability characterization of aluminium AA6082-O sheet metal by uniaxial tension and Erichsen cupping tests. *International Journal of Engineering and Technology*, 7(4):6768–6777, 2018.

[6] J. Adamus, M. Motyka, and K. Kubiak. Investigation of sheet-titanium drawability. In: *12th World Conference on Titanium (Ti-2011)*, Beijing, China, 19-24 June 2011.

[7] R.R. Goud, K.E. Prasad, and S.K. Singh. formability limit diagrams of extra-deep-drawing steel at elevated temperatures. *Procedia Materials Science*, 6:123–128, 2014. doi: 10.1016/j.mspro.2014.07.014.

[8] R. Norz, F.R. Valencia, S. Gerke, M. Brünig, and W. Volk. Experiments on forming behaviour of the aluminium alloy AA6016. *IOP Conference Series: Materials Science and Engineering*, 1238(1):012023, 2022. doi: 10.1088/1757-899X/1238/1/012023.

[9] W.S. Miller, L. Zhuang, J. Bottema, A.J. Wittebrood, P. De Smet, A. Haszler, and A. Vieregge. Recent development in aluminium alloys for the automotive industry. *Materials Science and Engineering: A*, 280(1):37–49, 2000. doi: 10.1016/S0921-5093(99)00653-X.

[10] J.C. Benedyk. Aluminum alloys for lightweight automotive structures. In P.K. Mallick (ed.): *Materials, Design and Manufacturing for Lightweight Vehicles*. Woodhead Publishing, pages 79–113, 2010. doi: 10.1533/9781845697822.1.79.

[11] M. Bloeck. Aluminium sheet for automotive applications. In J. Rowe (ed.): *Advanced Materials in Automotive Engineering*. Woodhead Publishing Limited, pages 85–108, 2012. doi: 10.1533/9780857095466.85.

[12] N.I. Kolobnev, L.B. Ber, L.B. Khokhlatova, and D.K. Ryabov. Structure, properties and application of alloys of the Al – Mg – Si – (Cu) system. *Metal Science and Heat Treatment*, 53(9-10):440–444, 2012. doi: 10.1007/s11041-012-9412-8.

[13] P. Lackova, M. Bursak, O. Milkovic, M. Vojtko, and L. Dragosek, Influence of heat treatment on properties of EN AW 6082 aluminium alloy. *Acta Metallurgica Slovaca*, 21(1):25–34, 2015. doi: 10.12776/ams.v21i1.553.

[14] R. Prillhofer, G. Rank, J. Berneder, H. Antrekowitsch, P. Uggowitzer, and S. Pogatscher. Property criteria for automotive Al-Mg-Si sheet alloys. *Materials*, 7(7):5047–5068, 2014. doi: 10.3390/ma7075047.

[15] N.C.W. Kuijpers, W.H. Kool, P.T.G. Koenis, K.E. Nilsen, I. Todd, and S. van der Zwaag. Assessment of different techniques for quantification of α-Al(FeMn)Si and β-AlFeSi intermetallics in AA 6xxx alloys. *Materials Characterization*, 49(5):409–420, 2002. doi: 10.1016/S1044-5803(03)00036-6.

[16] G. Mrówka-Nowotnik. Influence of chemical composition variation and heat treatment on microstructure and mechanical properties of 6xxx alloys. *Archives of Materials Science and Engineering*, 46(2):98–107, 2010.

[17] G. Mrówka-Nowotnik, J. Sieniawski, and A. Nowotnik. Tensile properties and fracture toughness of heat treated 6082 alloy. *Journal of Achievements of Materials and Manufacturing Engineering*, 12(1-2):105–108, 2006.

[18] G. Mrówka-Nowotnik, J. Sieniawski, and A. Nowotnik. Effect of heat treatment on tensile and fracture toughness properties of 6082 alloy. *Journal of Achievements of Materials and Manufacturing Engineering*, 32(2):162–170, 2009.

[19] X. He, Q. Pan, H. Li, Z. Huang, S. Liu, K. Li, and X. Li. Effect of artificial aging, delayed aging, and pre-aging on microstructure and properties of 6082 aluminum alloy. *Metals*, 9(2):173, 2019. doi: 10.3390/met9020173.

[20] Z. Li, L. Chen, J. Tang, G. Zhao, and C. Zhang. Response of mechanical properties and corrosion behavior of Al–Zn–Mg alloy treated by aging and annealing: A comparative study. *Journal of Alloys and Compounds*, 848:156561, 2020. doi: 10.1016/j.jallcom.2020.156561.

[21] J.R. Hirsch. Automotive trends in aluminium – the European perspective. *Materials Forum*, 28(1):15–23, 2004.

[22] W. Moćko and Z.L. Kowalewski. Dynamic properties of aluminium alloys used in automotive industry. *Journal of KONES Powertrain and Transport*, 19(2):345–351, 2012.

[23] N. Kumar, S. Goel, R. Jayaganthan, and H.-G. Brokmeier. Effect of solution treatment on mechanical and corrosion behaviors of 6082-T6 Al alloy. *Metallography, Microstructure, and Analysis*, 4(5):411–422, 2015. doi: 10.1007/s13632-015-0219-z.

[24] M. Fujda, T. Kvackaj, and K. Nagyová. Improvement of mechanical properties for EN AW 6082 aluminium alloy using equal-channel angular pressing (ECAP) and post-ECAP aging. *Journal of Metals, Materials and Minerals*, 18(1):81–87, 2008.

[25] I. Torca, A. Aginagalde, J.A. Esnaola, L. Galdos, Z. Azpilgain, and C. Garcia. Tensile behaviour of 6082 aluminium alloy sheet under different conditions of heat treatment, temperature and strain rate. *Key Engineering Materials*, 423:105–112, 2009. doi: 10.4028/www.scientific.net/KEM.423.105.

[26] O. Çavuşoğlu, H.İ. Sürücü, S. Toros, and M. Alkan, Thickness dependent yielding behavior and formability of AA6082-T6 alloy: experimental observation and modeling. *The International Journal of Advanced Manufacturing Technology*, 106:4083–4091, 2020. doi: 10.1007/s00170-019-04878-6.

[27] J. Slota, I. Gajdos, T. Jachowicz, M. Siser, and V. Krasinskyi. FEM simulation of deep drawing process of aluminium alloys. *Applied Computer Science*, 11(4):7–19, 2015.

[28] Ö. Özdilli. An investigation of the effects of a sheet material type and thickness selection on formability in the production of the engine oil pan with the deep drawing method. *International Journal of Automotive Science And Technology*, 4(4):198–205, 2020. doi: 10.30939/ijastech..773926.

[29] W.T. Lankford, S.C. Snyder, and J.A. Bauscher. New criteria for predicting the press performance of deep drawing sheets. *ASM Transactions Quarterly*, 42:1197–1232, 1950.

[30] A.C. Sekhara Reddy, S. Rajesham, and P. Ravinder Reddy. Evaluation of limiting drawing ratio (LDR) in deep drawing by rapid determination method. *International Journal of Current Engineering and Technology*, 4(2):757–762, 2014.

[31] R.U. Kumar. Analysis of Fukui's conical cup test. *International Journal of Innovative Technology and Exploring Engineering*, 2(2):30–31, 2013.

[32] Ł. Kuczek, W. Muzykiewicz, M. Mroczkowski, and J. Wiktorowicz. Influence of perforation of the inner layer on the properties of three-layer welded materials. *Archives of Metallurgy and Materials*, 64(3):991–996, 2019. doi: 10.24425/AMM.2019.129485.

[33] O. Engler and J. Hirsch. Polycrystal-plasticity simulation of six and eight ears in deep-drawn aluminum cups. *Materials Science and Engineering: A*, 452–453:640–651, 2007. doi: 10.1016/j.msea.2006.10.108.

[34] M. Koç, J. Culp, and T. Altan. Prediction of residual stresses in quenched aluminum blocks and their reduction through cold working processes. *Journal of Materials Processing Technology*, 174(1-3):342–354, 2006. doi: 10.1016/j.jmatprotec.2006.02.007.

[35] C.S.T. Chang, I. Wieler, N. Wanderka, and J. Banhart. Positive effect of natural pre-ageing on precipitation hardening in Al–0.44 at% Mg–0.38 at% Si alloy. *Ultramicroscopy*, 109(5):585–592, 2009. doi: 10.1016/j.ultramic.2008.12.002.

[36] S. Jin, T. Ngai, G. Zhang, T. Zhai, S. Jia, and L. Li. Precipitation strengthening mechanisms during natural ageing and subsequent artificial aging in an Al-Mg-Si-Cu alloy. *Materials Science and Engineering: A*, 724:53–59, 2018. doi: 10.1016/j.msea.2018.03.006.

[37] E. Ishimaru, A. Takahashi, and N. Ono. Effect of material properties and forming conditions on formability of high-purity ferritic stainless steel. Nippon Steel Technical Report. Nippon Steel & Sumikin Stainless Steel Corporation, 2010.

[38] E.H. Atzema. Formability of auto components. In R. Rana and S.B. Singh (eds.): *Automotive Steels. Design, Metallurgy, Processing and Applications*. Woodhead Publishing, pages 47–93, 2017. doi: 10.1016/B978-0-08-100638-2.00003-1.